HYDROTHERMALLY SYNTHESIZED NANOPARTICLES OF ZINC PEROXIDE AND THEIR STRUCTURAL DESCRIPTION

A. GARCÍA-RUIZ[1]*, A. ESCOBEDO[2], A. AGUILAR[3], R. ESPARZA[3] AND R. PÉREZ[3]

[1]UPIICSA-COFAA, Instituto Politécnico Nacional (IPN). Té 950, Col. Granjas-México, Iztacalco, 08400, México, D. F., México. [2]Instituto de Física, Benemérita Universidad Autónoma de Puebla (BUAP). A. P. J-48, Puebla, Pue., 72570, México. [3]Instituto de Ciencias Físicas, Universidad Nacional Autónoma de México (UNAM). P.O. Box 48-3, 62251, Cuernavaca, Mor., México. *E-mail: amado.garcia@gmail.com, Phone: +52 55 5796982.

Abstract

The aim of this work is to present some results of the synthesis of nanoparticles of zinc oxide by means of a hydrothermal method. Also, a description of the structural characteristics of these nanoparticles will be presented. The nanoparticles can be used as the supported active phase for photocatalytic applications, as has been recently published in the literature. The hydrothermal synthesis is based in dehydrated zinc acetate as the precursor using temperatures of 100 ºC. The structural analysis of the obtained nanoparticles has been performed using X-ray diffraction techniques with a subsequent Rietveld refinement of the pattern. This allows obtaining refined values of the cell parameters and the approximate crystallite sizes (10-20 nm) and also gives an insight on the morphology of the nanoparticle (truncated cube). Some high resolution electron microscope images are also presented and their structural results are compared with those obtained through the X-ray diffraction studies.

Keywords: Nanostructured oxides, hydrothermal synthesis, crystal structure, X-ray diffraction (XRD), transmission electron microscopy (TEM), crystallite morphology.

1. Introduction

Recently, there has been increasing interest in zinc peroxide (ZnO_2) and zinc oxide (ZnO), attracting the attention of many researchers because they have demonstrated to be very useful semiconductor materials with applications in rubber industry [1, 2], in the high-tech plastic processing [3], as an oxidant in explosives and pyrotechnic mixtures [4]. Zinc peroxide can also be useful in the cosmetic [5, 6] and pharmaceutical and therapeutic applications [6-9]. Stable nanoparticles of zinc peroxide can additionally be used as precursor for preparation of ZnO nanoparticles [10-13]. It is found that ZnO_2 nanoparticles decompose into ZnO at about 230 ºC and is stable up to 36 GPa at ambient temperature. With a great potential in applications, ZnO nanocrystals can be used as catalyst and photocatalyst [11, 14-17] and also in solar cells [18]. ZnO could be added to zeolites in order to improve their catalytic properties.

Nanocrystals, consisting of small crystallites of diameter < 100 nm, often have novel physical and chemical properties differing from those of the corresponding bulk materials [19]. The unique properties of nanocrystalline materials open up the general question of how crystallite size and shape affect the structural stability, and numerous efforts have been focused on controlling the sizes and shapes of inorganic nanocrystals, since they modify the surface area of the crystallites generally improving, among others, their catalytic properties. As mentioned above, they can be useful in many fields but little work has been done in some areas [9, 20]. Therefore, it is of great importance to produce high-quality ZnO_2/ZnO nanocrystalline materials for basic research as well as industrial and high-technology applications [21, 22]. Divers methods have been used in the preparation of zinc peroxide and zinc oxide, chemical and physical methods such as the hydrothermal one, laser ablation, sol–gel method precipitation in alcoholic medium, polyol synthesis, etc. In addition, other methods have been applied for the synthesis of ZnO nanostructures such as sputtering, molecular beam epitaxy, hydrothermal and electro-deposition [23-27]. In this work, nanocrystalline powders of zinc peroxide (ZnO_2), a precursor of zinc oxide (ZnO), have been prepared by means of a simple and low cost hydrothermal process of synthesis from zinc acetate dehydrates. These powders were structurally characterized having as propose to know their crystal size as well as their crystal shape. The powder samples were characterized mainly for running their X-ray diffraction patterns with a good statistic in order to calculate their crystallographic parameters by refining the pattern. Conditions of preparation and thermal treatment are related with the microstructure including nanocrystal size and shape. A pure cubic phase ZnO_2 was identified and after it was refined by using the Rietveld method to calculate some microstructural features of the nanocrystalline powders.

2. Experimental

In a typical synthesis 585.4 mg of zinc acetate dihydrate [$Zn(CH_3COO)_2 \cdot 2H_2O$, 99.6%, Baker] was dissolved in 80 ml of ultrapure deionized water (E-pure Barnstead system, 18 MΩ cm) under vigorous stirring until to obtain a transparent solution. After, 4 ml of hydrogen peroxide (H_2O_2 sol. 30%, Baker) was added. Then, the solution was heated up to 100 °C, and the hydrothermal reaction was conducted through 10 h. Once the solution was cooled to room temperature, the powder material was separated from the liquid phase by centrifugation and washed with deionized water several times. Structural and morphological characterization was performed by X-ray diffraction (XRD, Bruker Advance D-8) and transmission electron microscopy (TEM, Philips Tecnai F20, 200 kV, point resolution of 2.3 Å).

The X-ray powder diffraction pattern of ZnO_2 sample was recorded in θ–θ configuration at room temperature using CuKα radiation (1.5418 Å). Diffraction intensity was measured in the 2 of 10° - 110°; setting 0.02° and 4.0 s as step width and step counting time, respectively. The crystalline structure of the nanoparticles was refined through Rietveld method by means of FULLPROF98 code [28]. The diffraction peaks were fitted using pseudo-Voigt functions, the modified TCH (Thompson-Cox-Hastings) one [29], containing the refinable parameters related to average crystallite size and shape [30,31]. Sixteen variables were refined, including scale factor, refinable atom fractional coordinates, lattice parameters, isotropic thermal displacements, crystallite shape and size parameters, and values of strains. The modeled crystal structure was based in the available crystallographic data for cubic-ZnO_2 phase [32]. Finally, on using spherical harmonics functions, representative shape of the nanocrystallites was proposed.

TEM specimens were prepared by dispersing and subsequent drying a drop of solution on a copper grid (3 mm in diameter) covered with an amorphous carbon film. For comparison HREM simulated images have been obtained using the electron diffraction dynamical theory (multislice approach) [33] and some insights on the structural characteristic of nanometric ZnO_2 particle is withdrawn.

3. Results and discussion

Figure 1 shows the experimental and refined X-ray patterns of analyzed sample. The XRD pattern reveals the single phase and crystal structure of cubic-ZnO_2 nanoparticles (Space group: *Pa-3*, No. 205), all diffraction peak positions match with those reported in the JCPDS card No. 13-0311 for cubic-ZnO_2 powders. Since no appreciable difference of relative XRD peak intensities between our diffraction pattern and such reported for powder samples, it is suggested that neither texture or preferential orientation were induced in preparing the crystalline samples for XRD; also that none preferential growth is present in the nanopowders. No diffraction peak attributed to wurtzite-ZnO can be observed in XRD pattern of as-synthesized sample. These results, together with the slight broadening observed in the reflections, suggest that the synthesized sample is constituted by a collection of ZnO_2 nanocrystals, which was confirmed by TEM analysis, as it will be shown below.
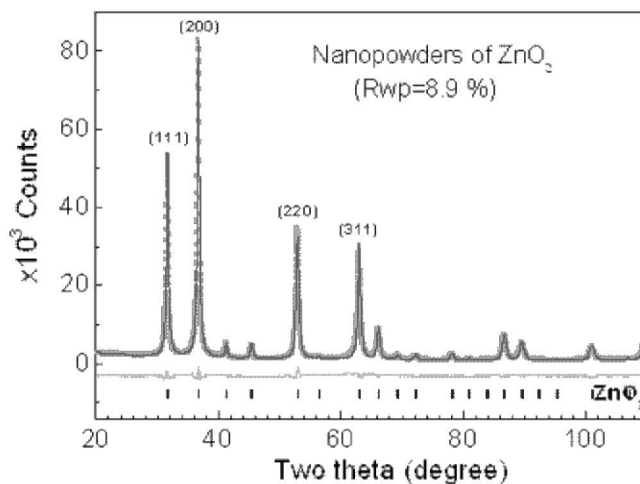

Figure 1. Experimental (green squares symbols) and calculated (continuous red line) XRD patterns of ZnO_2 nanopowder. The marks shown below indicate the XRD peak position of cubic ZnO_2 structure.

Table 1 shows the refined parameters calculated form Rietveld method. After the refinement procedure, the obtained values were: 4.89605(7) Å for the cubic lattice parameter a ($=b=c$), 15.4(6) nm for the average crystallite size and 18 % for the maximum microstrain. The fitting or quality of the refinement was measured by, among others, the residual function Rwp, which in these crystalline samples was around 8.9%.

Table 1. Refined cell parameters and calculated average particle size and maximum strain. Values indicating the goodness of the fitting were Rwp = 8.9, Chi2 = 13.0 and Rbragg = 3.6.

Space Group	Cell Parameter (Å)	Average Crystallite Size (nm)	Average Maximum Strain (%)
Pa-3 (No.205)	4.89605 (7)	15.4(6)	18(1)
Fractional Atomic Positions			
Atom	*x*	*y*	*z*
Zinc	0.0	0.0	0.0
Oxygen	0.4132(2)	0.4132(2)	0.4132(2)

With these microstructural results it is possible to draw a model structure of the cubic unit cell utilized to perform the refinement. Figure 2 shows the model of the cubic unit cell with the obtained parameters after refinement. This model, as known in the literature [32], is constituted by an array of irregular octahedra formed by a Zn ion at the center surrounded by four O ions located one at each corner of the polyhedron. It is important to mention that the atom positions undergo only a very small change with respect to the theoretical structure.
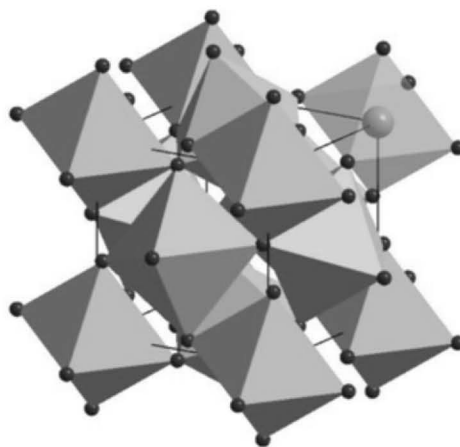

Figure 2. Schematic model of the cubic unit cell which has an octahedral oxygen structure and drawn with the refined lattice parameters (a=b=c=15.4(6) nm). Zn: gray circles in the center of each octahedron; O: small black circles.

On using the microstructural results summarized in table I, it also was possible to model the hydrothermally grown ZnO_2 nanoparticles, i. e., by using the known cubic cell model but with the precise parameters obtained in the synthesis and the refinement. Refinement procedure includes some parameters which can be used to simulate the shape and size of the crystallites which constitutes the powder sample. The reported size of the crystallite is an average of its diameter in all the planar directions in the crystallite. Shape of the particle is drawn with our software elaborated in the free programming text editor medit; it was made starting from a spherical model, the zero order, and modifying it from the inclusion of spherical harmonic of higher order. Series of spherical harmonics functions are applied to rebuild the shape of such representative nanocrystallite (Figure 3). It can be observed that the final shape of the simulated crystallite could be related with a truncated cube, where the surface planes are the (100) and the truncated ones are the (111). It is possible to appreciate relative similitude between the simulated morphology and the observed in TEM images.
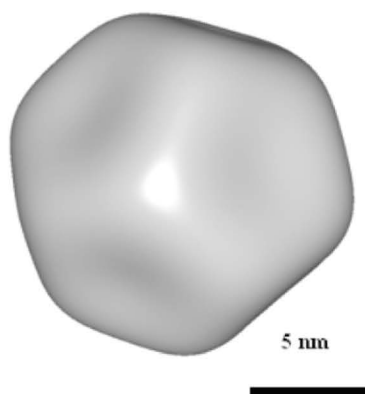
Figure 3. Proposed shape for synthesized ZnO$_2$ nanoparticles based in the calculated refined parameters.

Figure 4 finally shows some features of the nanopowders observed by transmission electron microscope. Insert 4a shows a characteristic HRTEM image from the ZnO$_2$ powders. The image resembles a small crystal with an average size of 10 nm, in agreement with calculated size using the Rietveld method. The ZnO$_2$ particles have cubo-octahedral shapes resulting from their fcc structure. The lattice distances 0.246 and 0.282 nm corresponding to the (020) and (111) plane of the cubic structure, respectively (JCPDS card No. 13-0311). The FFT (4b) shows the diffraction spots with zone axis along [101] direction, which indicates clearly the single-crystal feature of the powders. Insert 4c shows the HREM simulated image at the Scherzer's defocus (Δf = -424 Å). This image resembles the main image contrast characteristics of the experimental HREM image (4a). Insert 4d shows the supercell used for the simulation. It is interesting to observe that the nanocrystals, nearly spherical, have a faceted morphology however; this morphology could be related with the morphology of the proposed shape of the ZnO$_2$ nanocrystals (Figure 3). However, a more detailed HR-TEM analysis of the set of single ZnO$_2$ nanocrystals was not possible to do.
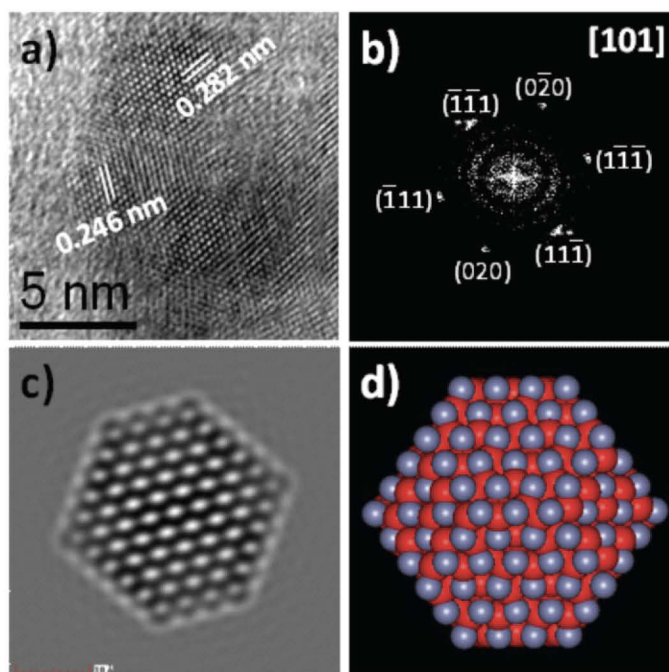

Figure 4. a) HR-TEM image of the as-grown ZnO$_2$ nanocrystal. b) FFT of the image shows the [101] zone axis of the nanocrystal. c) HREM simulated image at the Scherzer's defocus. This image resembles the main image contrast features of the experimental HREM image. d) Supercell used for the multislice simulation.

It will be necessary a study about the catalytic response of this material, however we can advance that the shape but especially the size in the nanometric regime, both features, increase the surface area and this should favor their catalytic properties.

4.   Conclusions

The hydrothermal chemical route is a facile, low cost and reliable method to synthesize high purity cubic-ZnO_2 nanoparticles, with faceted crystals and mean diameter of around 15 nm. Simulated morphology, structural properties and the unit cell parameters of synthesized cubic-ZnO_2 nanoparticles have been calculated using the Rietveld method. Use of this method in the characterization of these materials is the main aim of our work at this point. The obtained results are nearly consistent with those observed by means of transmission electron microscopy (TEM). We believed that, according with the cited literature, our ZnO_2 nanopowder can be easily used as precursor material to synthesize ZnO nanoparticles with similar morphology and size. This kind of morphologies and this nanosize offer a higher area for the catalytic activity of the material. Our work is right now addressed to study the catalytic behavior of the zinc nano-oxides specially by impregnating zeolites.

5.   References

[1] L. Ibarra, A. Marcos-Fernandez, M. Alzorriz, Polymer 43, 1649 (2002).

[2] L. Ibarra, J. Appl. Polym. Sci. 84, 605 (2002).

[3] S. Ohno, N. Aburatani, N. Ueda, DE Patent # 2914058 (1980).

[4] R. Hagel, K. Redecker, DE Patent # 2952069 (1981).

[5] M. Ceratelli, Zinc, Part 1. Fonderia (Milan) 43, 24 (1994).

[6] M. Farnsworth, C.H. Kline, J.G. Noltes, Zinc Chem. 248 (1973).

[7] D.A. Sunderland, J.S. Binkley, Radiology (Oak Brook, IL, United States) 35, 606 (1940).

[8] W. Klabunde, P.L. Magill, J.S. Reichert, US Patent # 2,304,104 (1942).

[9] L. Rosenthal-Toib, K. Zohar, M. Alagem, Y. Tsur, Chem. Eng. J. 136, 425 (2008).

[10] N. Uekawa, J. Kajiwara, N. Mochizuki, K. Kakegawa, Y. Sasaki, Chem. Lett. 7, 606 (2001).

[11] C. C. Hsu, N. L. Wu, J. Photochem. Photobiol. A 172, 269 (2005).

[12] M. Sun, W. Hao, C. Wang, T. Wang, Chem. Phys. Lett. 443, 342 (2007).

[13] Y. C. Zhang, X. Wu, X. Ya Hu, R. Guo, J. Cryst. Growth 280, 250 (2005).

[14] T. Szabó, J. Németh, I. Dékány, Colloids Surf. A: Physicochem. Eng. Aspects 230, 23 (2004).

[15] M.L. Curridal, R. Comparelli, P.D. Cozzli, G. Mascolo, A. Agostiano, Mater. Sci. Eng. C23, 285 (2003).

[16] V.P. Kamat, R. Huehn, R. Nicolaescu, J. Phys. Chem. B 106, 788 (2002).

[17] S.B. Park, Y.C. Kang, J. Aerosol Sci. 28, (1997).

[18] W.J.E. Beek, M. M. Wienk, R. A. J. Janssen, Adv. Funct. Mater. 16, 1112 (2006).

[19] Gleiter, H. Acta Mater. 48, 1 (2000).

[20] W. Chen, Y. H. Lu, M. Wang, L. Kroner, H. Paul, H.-J. Fecht, J. Bednarcik, K. Stahl, Z. L. Zhang, U. Wiedwald, U. Kaiser, P. Ziemann, T. Kikegawa, C. D. Wu, J. Z. Jiang, J. Phys. Chem. C 113, 1320 (2009).

[21] D.C. Look, Mater. Sci. Eng. B 80, 383 (2001).

[22] S.J. Pearton, D.P. Norton, K. Ip, Y.W. Heo, T. Steiner, Prog. Mater. Sci. 50, 293 (2005).

[23] M.N. Kamalasanan, S. Chandra, Thin Solid Films 288, 112 (1996).

[24] D. Jezequel, J. Guenot, N. Jouini, N.F. Fievet, J. Mater. Res. 10, 77 (1995).

[25] A.K. Chawla, D. Kaur, R. Chandra, Opt. Mater. 29, 995 (2007).

[26] K. Iwata, H. Tampo, A. Yamada, P. Fons, K. Matsubara, K. Sakurai, S. Ishizuka, S. Niki, Appl. Surf. Sci. 244, 504 (2005).

[27] M. Izaki, T. Omi, Appl. Phys. Lett. 68, 2439 (1996).

[28] J. Rodríguez-Carbajal, Laboratoire Leon Brillouin (CEA-CNRS), France.

[29] P. Thompson, D.E. Cox, J.B. Hasting. J. Appl. Crystallogr. 20, 79 (1987).

[30] R.A. Young, P. Desai. Arch. Nauki Mater. 10, 71 (1989).

[31] E. Prince. J. Appl. Crystallogr. 14, 157 (1981).

[32] N.G. Vannerberg, Arkiv foer Kemi 14, 19 (1959).

[33] A. Gomez, Micr. Re. Technol. 40, 37 (1998).